2017

N-isopropylacrylamide-based Photopolymer for Holographic Recording of Thermosensitive Transmission and Reflection Grating

Tatsiana Mikulchyk
Technological University Dublin, t.mikulchyk@gmail.com

Suzanne Martin
Technological University of Dublin, suzanne.martin@tudublin.ie

Izabela Naydenova
Technological University Dublin, izabela.naydenova@tudublin.ie

Recommended Citation

MIkulchyk, T., Martin, S. & Naydenova, I. (2017). N-isopropylacrylamide-based photopolymer for holographic recording of thermosensitive transmission and reflection gratings. *2017 52nd International Universities Power Engineering Conference (UPEC)*,Technological Educational Institute of Crete (TEI of Crete) Stauromenos Heraklion, Crete, Greece, 28 - 31 Aug 2017. doi:10.1109/UPEC.2017.8231983

N-isopropylacrylamide-based photopolymer for holographic recording of thermosensitive transmission and reflection gratings

Tatsiana Mikulchyk, Suzanne Martin, Izabela Naydenova*

Centre for Industrial and Engineering Optics, School of Physics, College of Sciences and Health, Dublin Institute of Technology, Kevin Street, Dublin, D08 NF82, Ireland
**Corresponding author: izabela.naydenova@dit.ie*

Received XX Month XXXX; revised XX Month, XXXX; accepted XX Month XXXX; posted XX Month XXXX (Doc. ID XXXXX); published XX Month XXXX

In recent years, functionalized photopolymer systems capable of holographic recording are in great demand due to their potential use in the development of holographic sensors. This work presents a newly developed *N*–isopropylacrylamide(NIPA)-based photopolymer for holographic recording in reflection and transmission modes. The optimized composition of the material is found to reach refractive index modulation of up to 5×10^{-3} and 1.6×10^{-3} after recording in transmission and reflection mode, respectively. In addition to fulfilling the requirements for holographic recording materials, the NIPA-based photopolymer is sensitive to temperature and has lower toxicity than acrylamide-based photopolymers. Possible application of the NIPA-based photopolymer in the development of a holographic temperature sensor is discussed.

OCIS codes: *(090.0090) Holography, (090.7330) Volume gratings, (050.1950) Diffraction gratings, (130.6010) Sensors, (350.5130) Photochemistry.*

1. INTRODUCTION

Functionalized photopolymer systems capable of holographic recording are of particular interest due to their potential to be utilized in the development of holographic sensors. These devices are able of providing real-time, reversible or irreversible, visual colorimetric or optical readouts [1,2]. The basic holographic sensor consists of a holographic diffraction grating embedded in the functionalized photopolymer system. Upon interaction with the analyte, the analyte-responsive film acts as a recognition component and provides changes in holographic grating properties such as the peak wavelength of the diffracted light, the diffraction efficiency and the Bragg angle. Functionalized photopolymer systems must have both good holographic recording characteristics and the response to a specific analyte. The simplest way to design a holographic recording material responsive to a specific analyte is based on exploitation of the intrinsic properties of the material. The intrinsic properties can be varied by incorporation of components with sensitivity to a specific analyte.

This work focuses on a temperature sensitive holographic material and its application for the development of holographic temperature sensors operating in the temperature range from 18 to 50 °C. Among a large variety of sensors, temperature sensors are in great demand as temperature control is necessary in a wide range of industrial processes [3]. Holographic diffraction grating based temperature sensors have an advantage over other optical temperature sensors as the holographic technique allows rapid production of lightweight, miniature and disposable sensors [4-8].

Previously, the concept of a switchable diffraction grating was demonstrated and switchable volume reflective elements were fabricated from a polymer liquid crystal polymer slice structure by holographic photopolymerization [9-13]. Capacity to control the reflection efficiency is based on refractive index modulation change induced by electric field or temperature. In the present research, temperature-controlled refractive index modulation of the photopolymer-based holographic gratings is implemented for the development of holographic temperature sensors.

The aims of the present research are the development of the temperature sensitive photopolymer composition capable of recording both transmission and reflection holograms and characterization of the temperature response of holographic gratings recorded in this photopolymer composition.

2. PHOTOPOLYMER COMPOSITION

Our approach is based on introducing a thermosensitive monomer such as *N*–isopropylacrylamide as the main monomer in order to create a temperature sensitivity of the material. The temperature sensitivity of Poly(*N*–isopropylacrylamide) (PNIPA) is derived from its capability to undergo phase transition at a critical temperature. PNIPA can be classified as a negative temperature-sensitive system and has a lower critical solution temperature (LCST) of about 32°C, which can be manipulated by copolymerization of NIPA with other appropriate monomers [14]. In addition of temperature sensitivity, PNIPA has an advantage such as low toxicity [15,16]. Due to its low toxicity PNIPA is the most popular intelligent polymer used for the development of temperature responsive materials for drug delivery, tissue engineering, biosensors etc. [17-22].

Also, our innovation step includes the incorporation of *N*–phenylglycine (NPG) as a photoinitiator. The utilization of NPG instead of traditionally used triethanolamine as the primary photoinitiator allows decreasing the permeability of the layer to water molecules and improves both the humidity resistance of the holographic grating and the scratch resistance of the photopolymer layer [23]. At the same time it has been demonstrated that holographic diffraction gratings recorded in photopolymer systems

containing NPG as the initiator suffer from the lower diffraction efficiency [23,24].

During the development of the photopolymer composition introduced in the present paper, the diffraction efficiency was found to decrease up to two times within few hours after the recording. Deterioration of the diffraction efficiency was attributed to the low diffusion rate of monomers. The low diffusion rate of monomers led to the significant amount of unreacted monomers remaining in dark regions after the recording. Due to the concentration gradient created during the holographic recording, the monomers diffused from dark to bright regions causing the refractive index modulation reduction and, as a result, the diffraction efficiency decreased.

In order to stabilize the diffraction efficiency, glycerol as a plasticizer was introduced into the photopolymer composition. As shown previously [25], the addition of glycerol promotes diffusion of monomer molecules during holographic recording, improves exposure sensitivity and the stability of created photonic structures. After addition of glycerol, the stability of the diffraction efficiency of gratings recorded in the NIPA-based photopolymer composition was improved. In transmission gratings, the diffraction efficiency was unchanged within 14 days and 30 % decrease was noticed in 21 months. In reflection gratings, a few percent decay of the diffraction efficiency was observed within 24 hours after the recording. After 41 days a 20 % decrease was noticed. To prevent the observed decay of the diffraction efficiency, reflection gratings were UV-cured using Dymax UV curing system (model ECE-200). After UV-curing with total exposure of 5.4 J/cm^2 the decrease for few percent was observed within 41 days after the recording. Thus, the addition of glycerol followed by UV-curing allowed stabilizing photonic structures holographically recorded in the NIPA-based photopolymer.

Optimization of the photopolymer formulation was carried out by varying the concentration of all the constituent elements in order to create a photopolymer material with good holographic recording characteristics. The alteration of the monomer concentration allowed determining the maximum amount of monomers, which can be accommodated by the matrix without phase separation. The saturated amount of NIPA in the photopolymer solution is found to be ~11 mg/ml. Introducing higher amount of NIPA leads to the deterioration of the layer quality, i.e. crystallization of NIPA on the surface of the layer. According to the previous research [26], the best performance of the NIPA-based photopolymer was observed when the ratio of NIPA and the cross-linker such as *N, N'*–methylenebisacrylamide (BA) was 4:3. In our research, the NIPA and BA ratio was also kept 4:3.

Then, the optimization of the photoinitiating system was carried out to improve the sensitivity of the material. The optimum concentrations of the light absorbing component (Erythrosin B) and NPG were obtained by determining the maximum achievable refractive index modulation during holographic recording. Finally, the glycerol concentration was optimized. In transmission mode, the optimum concentration of glycerol was determined as minimum concentration that allowed recording gratings with stable diffraction efficiency within 14 days and it was 0.2 ml in 18.2 ml of the photopolymer solution.

In reflection mode, the material should be able to achieve high spatial resolution. Spatial resolution can be manipulated by controlling the size of polymer chains during its growing and extending out/diffusing into the illuminated areas. To improve the spatial resolution of the material, recently proposed approach [27] was utilized. It was observed [27] that the combination of the chain transfer agent (CTA), such as citric acid, with the free radical scavenger, such as glycerol, improved the spatial resolution of the photopolymer material and led to enhancement of the diffraction efficiency. Based on this approach, two modifications of the NIPA-based photopolymer composition were done. Firstly, CTA such as citric acid was incorporated. Secondly, glycerol concentration was increased in comparison with the photopolymer composition for the transmission mode recording. CTA terminates the polymer chain and forms a new active radical capable of initiating the growth of a new polymer chain [28]. This promotes the growth of shorter polymer chains and prevents their extending out of the bright fringe areas leading to the higher refractive index modulation and, hence, the diffraction efficiency. At the same time, shorter chains are more mobile and can diffuse from the bright to dark regions [29,30]. In order to limit the mobility of short chains, the concentration of glycerol was increased. Glycerol speeds up polymerization leading to decreased permeability of the matrix and limited mobility of short chains. The improvement of spatial resolution and diffraction efficiency can be explained by the effects of both CTA, which promotes the growth of shorter chains, and glycerol, which restrict short polymer chain movement [27]. Our experimental results showed that the increase of glycerol concentration from 0.2 ml to 1 ml allowed enhancing the diffraction efficiency of the reflection grating from 6 to 20 %. In addition, polyvinyl alcohol with low level of hydrolysis (80 %) was used as it had been found to have low permeability that allowed recording in reflection mode [31].

The optimized photopolymer composition is presented in Table 1. The composition of the thermosensitive photopolymer for recording in transmission mode contains an inert polymeric binder (polyvinyl alcohol, molecular weight of 9000-10000, 80 % hydrolyzed, Sigma Aldrich), a monomer (*N*–isopropylacrylamide, 97 %, Sigma Aldrich), a cross-linker (*N, N'*–methylenebisacrylamide, 99 %, Sigma Aldrich), a photo-initiator (*N*–phenylglycine, 97 %, Sigma Aldrich), a plasticizer and a free radical scavenger (glycerol, 98 %, Fisher Scientific) and a light absorbing component (Erythrosin B, Sigma Aldrich). The composition for recording in reflection mode also contains CTA such as citric acid (99 %, Sigma Aldrich). The newly developed photopolymer composition is a self-processing material, which does not require any post treatment in order to develop a volume phase transmission/reflection grating.

Table 1. Photopolymer Composition

Chemical Reagent	Chemical Compound	Transmission Mode	Reflection Mode
Polyvinyl alcohol		8.79 % w/v	8.42 % w/v
N–isopropyl acrylamide		0.097 M	0.093 M
N, N'–Methylene bisacrylamide	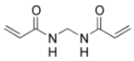	0.053 M	0.051 M
Erythrosin B	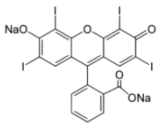	1.37×10^{-4} M	1.32×10^{-4} M
N–phenylglycine		0.0145 M	0.0139 M
Glycerol	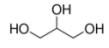	0.15 M	0.72 M
Citric acid	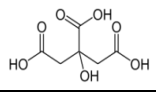	-------	0.022 M

3. EXPERIMENTAL

3.1. Holographic Recording

The photopolymer solution was prepared by mixing all the components using a magnetic stirrer. Photopolymer layers with the thickness varying from 20 to 115 μm were prepared by deposition of the appropriate amount of photopolymer solution on the leveled glass slides (76 × 26 mm^2) and drying for 18 hours in a dark room at temperature of 21 ± 2 °C and the relative humidity of 35 ± 5 %. In order to get 100 μm thick layers, 3 ml and 1.5 ml of photopolymer solution for recording in transmission and reflection modes, respectively, were used. The thickness of the dry layers was measured with a white light interferometric surface profiler MicroXAM S/N 8038.

The transmission and reflection volume phase gratings were recorded using the set-up presented in Figure 1a and 1b, accordingly. The photopolymer layers were exposed to two beams of 532 nm wavelength obtained by splitting a Nd:YVO$_4$ laser beam. Holographic recordings were done at 532 nm wavelength as it was previously demonstrated that the maximum absorbance of the photopolymer composition sensitized with Erythrosin B was 526 nm [32]. In order to achieve the best performance of the photopolymer composition, the recording conditions were optimized by varying the recording time and total recording intensity. The results from the holographic characterization of the photopolymer composition are presented in section 4.

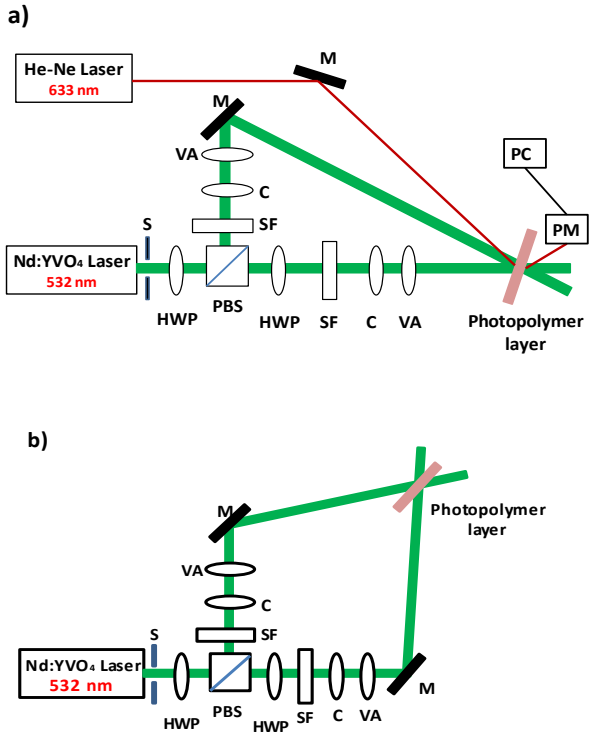

Fig. 1. Experimental set-up for the recording of a transmission grating (a) and a reflection grating (b): S - electronic shutter; HWP – half-wave plate; PBS – polarizing beam splitter; SF – spatial filter; C – collimator; VA - variable aperture; M – mirror; PM – power meter; PC - computer.

In transmission mode recording, the angle of the recording beams was altered to record diffraction gratings with the spatial frequency of 300, 1000 and 2700 lines/mm. Real-time diffraction efficiency growth curves were recorded using a 633 nm probe beam from He–Ne laser. The intensity of the diffracted beam was monitored by means of an optical power meter (Newport 1830-C) and the acquired data were transferred to a computer. The diffraction efficiency of the transmission gratings was calculated as the ratio of the intensity of the diffracted beam and the intensity of the incident beam.

In reflection mode recording, diffraction gratings with the spatial frequency of approximately 2700 lines/mm were recorded. The diffraction efficiency was monitored using a 532 nm beam from Nd:YVO$_4$ laser and was determined as the ratio of the intensity of the diffracted beam and the difference of the intensities of the incident beam and the reflected beam.

Quantitative analysis of the refractive index modulation (Δn) of the material achieved during holographic recording was carried out using the coupled wave theory [33]. The applicability of the coupled wave theory was justified by calculation of Q factor using Equation (1) [34]:

$$Q = \frac{2\pi\lambda d}{n\Lambda^2}, \tag{1}$$

where λ is the wavelength of the recoding light, d is the thickness of the photopolymer layer, n is the average refractive index of the medium and Λ is the spatial period. In the present research, Q factor for the transmission gratings with the spatial frequency of 300 lines/mm and with the thickness ranging from 30 to 90 μm was found to be in the range from 6 to 18. For the reflection gratings with the spatial frequency of 2700 lines/mm and thickness ranging from 20 to 115 μm, Q factor was estimated to be in the range from 326 to 1878. This allowed applying the coupled wave theory for the evaluation of the refractive index modulation achieved during holographic recording. Equations (2) and (3) were utilized for transmission mode and reflection mode, respectively:

$$\Delta n = \frac{\lambda \cos\theta \sin^{-1}\left(\sqrt{\eta}\right)}{\pi d}, \tag{2}$$

$$\Delta n = \frac{\lambda \cos\theta \tanh^{-1}\left(\sqrt{\eta}\right)}{\pi d}, \tag{3}$$

where λ is the wavelength of the reconstructing beam, θ is the Bragg angle inside the photopolymer layer for the reconstructing wavelength, η is the diffraction efficiency.

3.2. Temperature Response Testing

Before the temperature test, the gratings were UV-cured by exposing them to 5.4 J/cm^2 using Dymax UV-curing system. It was carried out in order to polymerize all residual monomers and to stabilize the recorded gratings. The temperature response of the transmission grating was investigated by monitoring the maximum diffraction efficiency in the temperature range from 18 to 47 °C and at relative humidity of 60 %. In order to monitor the maximum diffraction efficiency, the position of the sample at every temperature was adjusted by rotation and the diffraction efficiency at Bragg incidence was obtained. A controlled environment chamber with humidity and temperature control system (Electro-tech system, model 5503-11) was used in order to create different environmental conditions. During the exposure to temperature, the intensities of transmitted (I_0) and the first-order diffracted (I_1) beams were monitored by means of an optical power meter (Newport 1830-C) simultaneously (Figure 2a). The readings were taken 5 min after exposure to a new temperature to allow for the samples to equilibrate with the surrounding conditions and the diffraction efficiency in this experiment was defined as $I_1/(I_1+I_0)$.

The temperature response of the reflection grating was characterized by monitoring the peak wavelength of the light diffracted by the diffraction grating in the temperature range from 20 to 50 °C and at relative humidity of 60 % (Figure 2b). The probe light from a broadband light source (AvaLight HAL-S) was guided into the chamber by a fibre optic cable (Avantes FC-UV400-2). The diffracted light from the grating was coupled through a second fibre optic cable to a spectral analyzer (Avantes AvaSpec-2048). The readings were taken 5 min after exposure to the new temperature in order to allow the samples to equilibrate with the surrounding conditions.

4. HOLOGRAPHIC PERFORMANCE OF THE NIPA-BASED PHOTOPOLYMER

4.1. Diffraction Efficiency

The holographic recording capabilities of the NIPA-based photopolymer were investigated by recording transmission volume phase gratings at the spatial frequency of 300, 1000 and 2700 lines/mm and reflection volume phase gratings at the spatial frequency of 2700 lines/mm. Optimized conditions for the recording in both transmission and reflection modes are shown in Table 2.

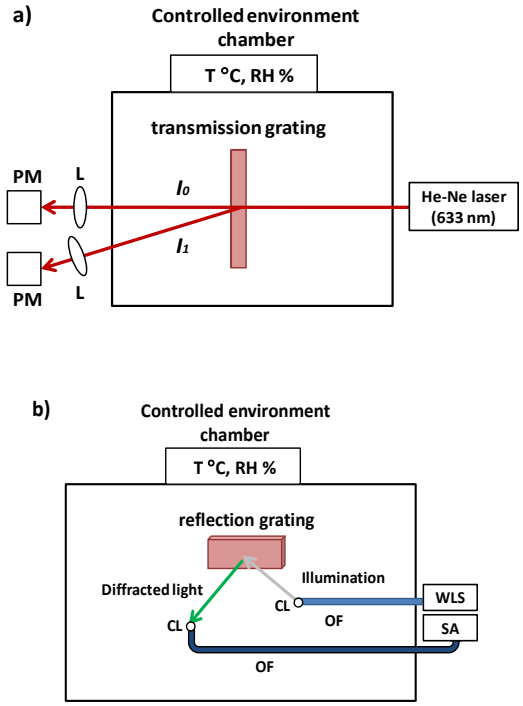

Fig. 2. Schematic representation of the set-up for testing the temperature response of the transmission grating (a) and the reflection grating (b). L – lens; PM – power meter; CL – collimating lens; OF – optical fibre; WLS – white light source; SA – spectral analyzer.

Table 2. Holographic Recording Characteristics

Recording Mode	Spatial Frequency (lines/mm)	Optimum Total Recording Intensity (mW/cm^2)	Total Exposure (mJ/cm^2)	Diffraction Efficiency (%) [60 ±5 μm thick layer]
Transmission	300	2.0	700	60
Transmission	1000	2.0	320	80
Transmission	2700	9.5	600	30
Reflection	2700	10.5	1050	20

Figure 3a presents the phase-contrast microscopy image of the photonic structure recorded in transmission mode at a spatial frequency of about 300 lines/mm in the NIPA-based photopolymer. The image displays the map of the refractive index in the recorded area. Figure 3b shows the profile of the refractive index modulation created during holographic recording. The intensity of the signal is the transmittance of the sample, which corresponds to the refractive index in the recorded area. It is observed that the intensity changes periodically with a spatial period of about 3 μm which confirms that the spatial frequency of the recorded photonic structure is about 300 lines/mm.

Figure 4 shows typical diffraction efficiency growth curves for transmission gratings with the spatial frequency of 300, 1000 and 2700 lines/mm recorded using total recording intensities presented in Table 2. The thickness of the layer was 60 ± 5 μm. The photoresponse of the material is nonlinear due to complicated processes of polymerization and diffusion resulting in the refractive index variation. The slope of its linear part gives the sensitivity of the material that depends on the spatial frequency. At 300 lines/mm and 1000 lines/mm total recording intensity of 2 mW/cm^2 was found to be the optimum to get maximum diffraction efficiency using minimum exposure. The diffraction efficiency of 60 % and 80 % was achieved for transmission gratings with spatial frequency of 300 lines/mm and 1000 lines/mm in 60 ± 5 μm thick layers, respectively. At 2700 lines/mm the diffraction efficiency of 30 % was reached after 63 seconds of exposure to the total recording intensity of 9.5 mW/cm^2.

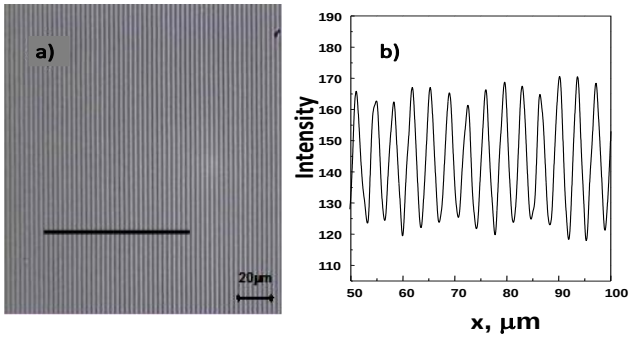

Fig. 3. Phase-contrast microscopy image (a) and refractive index modulation profile (b) of the photonic structure with a spatial frequency of 300 lines/mm recorded in the NIPA-based photopolymer.

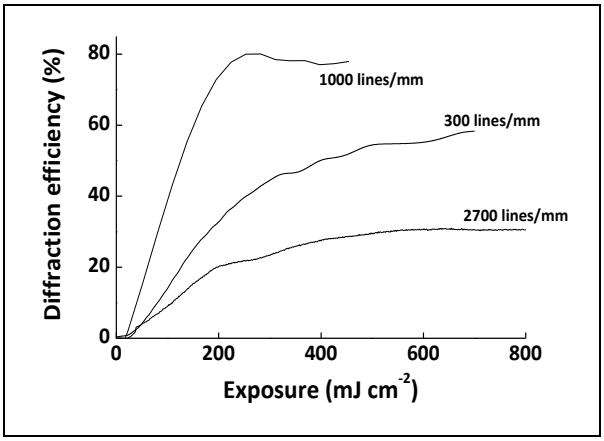

Fig. 4. Diffraction efficiency growth curves for transmission gratings with the spatial frequency of 300 lines/mm, 1000 lines/mm and 2700 lines/mm.

Figure 5 shows angular selectivity curves of transmission gratings with the spatial frequency of 300, 1000 and 2700 lines/mm recorded in the photopolymer layers with the thickness of 75 ± 5 μm. Angular selectivity curves of transmission gratings have the side lobes indicating uniformity of the refractive index profile through the depth of the photopolymer layer created during holographic recordings [35].

To record high quality holograms in reflection mode, materials with high spatial resolution are required. As discussed above, the photopolymer composition was modified by incorporation of citric acid as a chain transfer agent which in combination with glycerol (a free radical scavenger) improved the spatial resolution of material. Once the concentration of the citric acid was optimized, volume phase reflection gratings with the spatial frequency of 2700 lines/mm were

recorded in 60 ± 5 μm thick layers. Optimum total recording intensity was found to be 10.5 mW/cm². Experimental dependence of the diffraction efficiency on the exposure energy is presented in Figure 6.

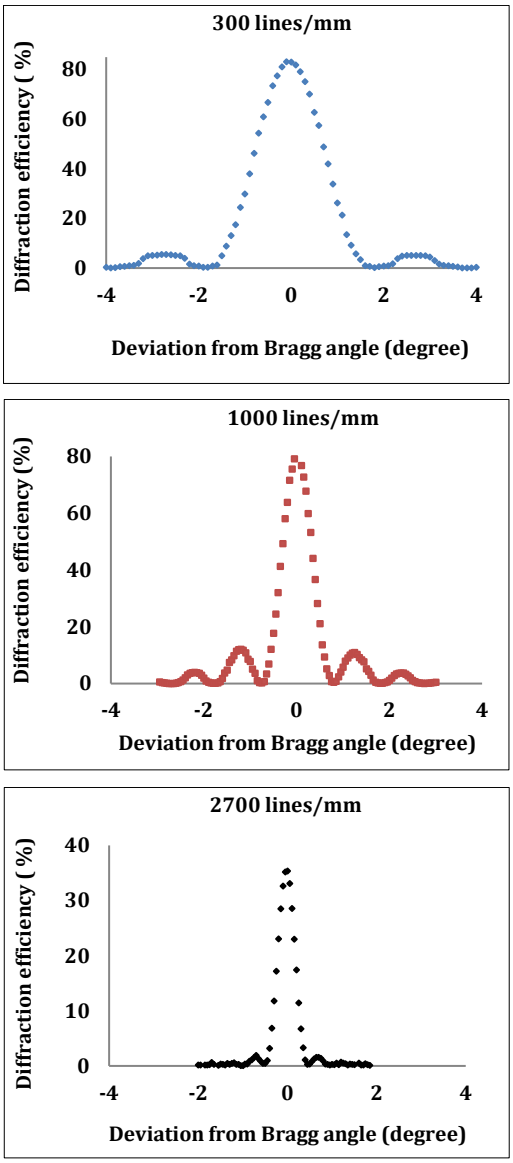

Fig. 5. Angular selectivity curves for transmission gratings with the spatial frequency of 300 lines/mm, 1000 lines/mm and 2700 lines/mm.

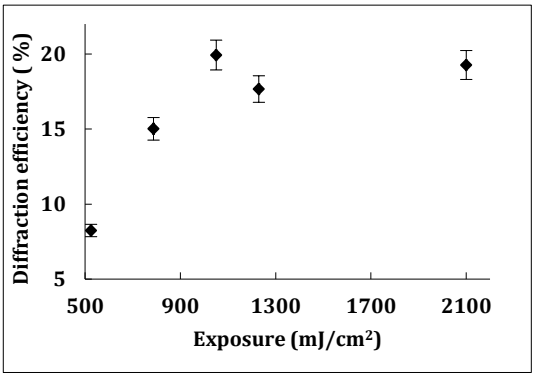

Fig. 6. The diffraction efficiency of reflection gratings with the spatial frequency of 2700 lines/mm versus exposure.

The diffraction efficiency of 20 % was obtained for the exposure energy of 1050 mJ/cm². Further increase of the exposure energy up to two times did not lead to the improvement of the diffraction efficiency. A possible explanation is that at the exposure energy of 1050 mJ/cm² the available dynamic range of the material has been used up fully. This assumption is also supported by the experimental data on UV-curing. The diffraction efficiency of sample recorded with the exposure energy of 1050 mJ/cm² is found to remain unchanged after UV-curing with total exposure of 5.4 J/cm².

Thus, the NIPA-based photopolymer is capable of holographic recording in both transmission and reflection modes and the diffraction efficiency of 80 % and 20 % can be reached, respectively.

4.2 Refractive Index Modulation

Refractive index modulation achieved during holographic recoding is one of the most important parameters of a holographic recording material. Characterization of the refractive index modulation in the NIPA-based photopolymer was carried out for both transmission and reflection recording modes. Experimental results for transmission gratings recorded at the spatial frequency of 300, 1000 and 2700 lines/mm in the layers with the thickness ranging from 30 to 90 μm are shown in Figure 7.

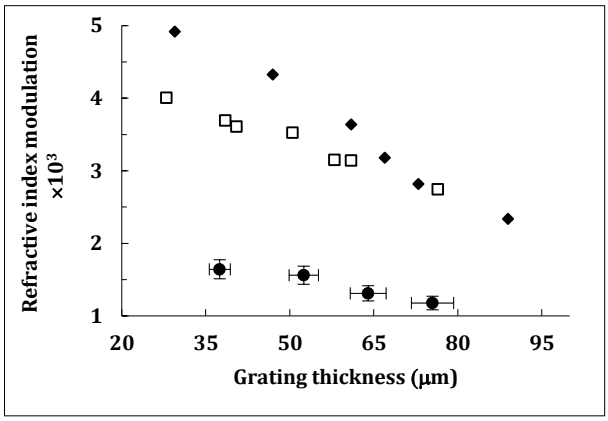

Fig. 7. Refractive index modulation versus the thickness of transmission gratings recorded at the spatial frequency of 300 lines/mm (□), 1000 lines/mm (♦) and 2700 lines/mm (●).

The photoinduced refractive index modulation was found to depend on the thickness and the spatial frequency of the grating. The decrease of the refractive index modulation with increasing thickness was observed. Possible reasons are the material absorption and the scattering of the incident light beams. These effects become more pronounced in the thick layers leading to the incident light intensity losses and the decrease of the refractive index modulation. This could lead to attenuation of the grating inside the photopolymer layer [36,37]. Also, the refractive index modulation depends on the spatial frequency. Maximum refractive index modulation of up to 5×10^{-3} was reached after holographic recording in 30 ± 2 μm thick layers at 1000 lines/mm. The refractive index modulation at 2700 lines/mm was significantly less due to limited resolution of the material. For applications where high diffraction efficiency is required at the spatial frequencies in the range from 2000 to 3000 lines/mm the photopolymer composition containing citric acid and increased concentration of glycerol can be used.

Figure 8 shows the dependence of the refractive index modulation versus the grating thickness for holographic recordings of reflection volume phase gratings with the spatial frequency of 2700 lines/mm. The decrease of the refractive index modulation with increasing thickness was observed due to light absorption in the photopolymer layer. The thicker the layer, the bigger the difference in intensity of the two recording beams. This leads to the lower visibility of interference fringes during holographic recording and, hence, the lower refractive index modulation is achieved. The new material was found to reach refractive index modulation of up to 1.6×10^{-3} in 20 ± 2 μm thick layers and up to 0.6×10^{-3} in 115 ± 5 μm thick layers. Optical thickness

in 532 nm was found to be 1.8 and 3.5 for the layers with the thickness 50 and 95 μm, respectively. Thus, the refractive index modulation of the material can be tuned by the alteration of the thickness of the layer. This is beneficial for the utilization of novel photopolymer in diffractive optics.

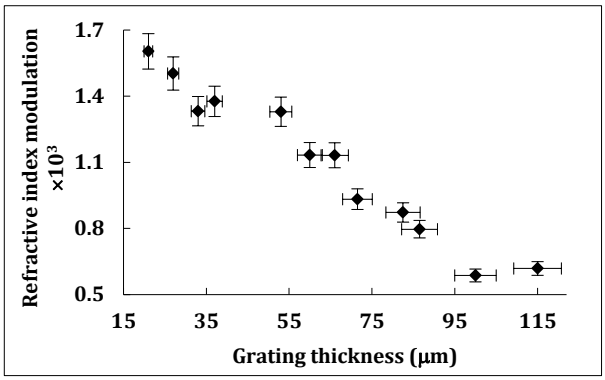

Fig. 8. Refractive index modulation versus the thickness of reflection gratings recorded at the spatial frequency of 2700 lines/mm.

5. TEMPERATURE RESPONSE

5.1. Transmission Gratings

The temperature response of transmission gratings with the spatial frequency of 1000 lines/mm was investigated by monitoring the maximum diffraction efficiency in the temperature range from 18 to 47˚C and at relative humidity of 60 %. Transmission gratings with initially low diffraction efficiency of 35 ± 2 % were recorded in 60 ± 5 μm thick layers using exposure time of 40 sec and total exposure intensity of 2 mW/cm². Normalized diffraction efficiency was calculated as the ratio of the diffraction efficiency at certain temperature and the diffraction efficiency at the start of the experiment at 18˚C. The dependence of normalized diffraction efficiency on temperature is presented in Figure 9.

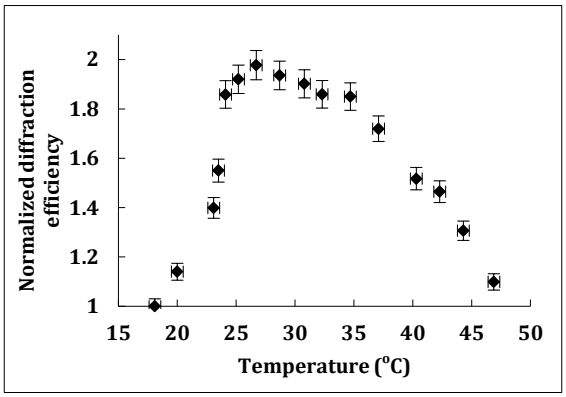

Fig. 9. Temperature dependence of normalized diffraction efficiency of the transmission grating.

When the temperature increases, the diffraction efficiency increases at temperatures below 30˚C and decreases above 30˚C. Such behavior of the diffraction efficiency can be explained by means of the ability of the photopolymer layer to transit from the hydrophilic state to the hydrophobic state at a critical temperature. The temperature level at which changes in the behavior observed is close to the LCST of PNIPA. At temperatures below 30˚C the photopolymer layer is hydrophilic. As known, the higher the temperature, the higher the concentration of water molecules in the air at certain humidity level. The higher the temperature the more water molecules are absorbed by the layer leading to the increase of both the grating thickness and the refractive index modulation. At temperatures above 30˚C the photopolymer layer is getting hydrophobic and the absorbed water is expelled leading to the decrease of the diffraction efficiency due to the shrinkage of the layer and the decrease of the refractive index modulation.

Thus, the sensing capability of the transmission grating recorded in the NIPA-based photopolymer composition is based on temperature-induced changes in the diffraction efficiency. The transmission holograms produced in this photopolymer composition can be used for the development of holographic temperature sensors and temperature switchable attenuators.

5.2. Reflection Gratings

The temperature response of the reflection grating with the spatial frequency of 2700 lines/mm was characterized by monitoring the peak of the wavelength of the diffracted light in the temperature range of 20 - 50˚C and at relative humidity of 60 % (Figure 10). Total recording intensity of 10.5 mW/cm² and exposure energy of 1050 mJ/cm² were used to record the reflection grating in 60 ± 5 μm thick layers.

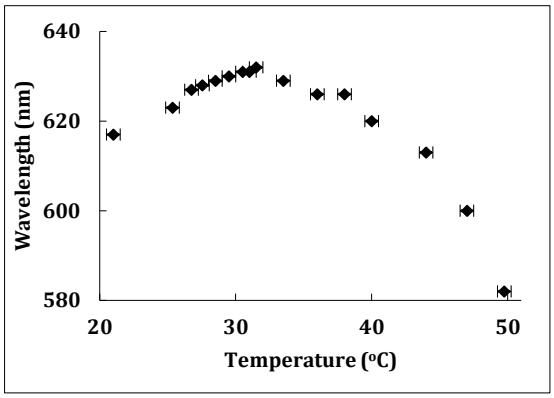

Fig. 10. Spectral response of the reflection grating versus temperature.

The trend of the temperature response of the reflection grating is similar to one of the transmission grating. Exposure to temperature below 30˚C causes the swelling of the photopolymer layer leading to the increase of the grating period and the wavelength shift of up to 15 nm to longer wavelength. Exposure to temperature above 30˚C induces the shrinkage of the layer leading to the decrease of the grating period and as a result the wavelength shifts to shorter wavelengths for up to 50 nm. The wavelength shift of 50 nm can be visually detected by a color change of the hologram when reconstructed in white light. Figure 11 demonstrates the photographs of the key and its Denisyuk hologram recorded in the NIPA-based photopolymer. Denisyuk hologram was recorded in 60 ± 5 μm thick layers using the recording intensity of 25 mW/cm² and exposure time of 100 sec. Figure 11b and 11c show holograms of the key before exposure to temperature (at 20˚C) and during exposure to temperature of 50˚C, respectively.

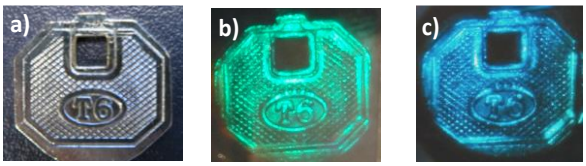

Fig. 11. The photographs of the key (a) and its Denisyuk hologram recorded in the NIPA-based photopolymer before temperature exposure (b) and during exposure to temperature of 50˚C (c).

It can be seen that the temperature increase from 20˚C to 50˚C causes a color change of the hologram. This is well suited to the application of reflection holograms as temperature visual indicators that visibly change the color under temperature exposure. The

reversibility of the temperature induced wavelength shift was studied by exposing the reflection grating to 6 cycles of temperature changes. The wavelength shift caused by temperature exposure for identical period of time was observed to be constant. However, the wavelength of the diffracted light was found to not recover to its initial value. After recovery for 24 hours at 20˚C the wavelength of the diffracted light shifted to the shorter wavelength for 5 nm. The possible explanation can be potential inability of the matrix to recover to the original volume.

Thus, the temperature response of the reflection diffraction grating recorded in NIPA-based photopolymer composition is based on changes in the peak wavelength of the diffracted light due to the spatial period alterations caused by temperature induced conformational changes of PNIPA molecules at a critical temperature. Possible application of reflection holograms is temperature sensitive labels that indicate what the current temperature of the product is and especially if it is above a temperature that is critical for protecting the quality of the goods. Such product will be very useful for packaging industry where goods need to be stored at specific temperature and not exceed it.

6. CONCLUSION

The NIPA-based photopolymer composition for holographic recording in transmission and reflection modes has been developed. Replacing toxic and carcinogenic acrylamide with low-toxic *N*–isopropylacrylamide allows decreasing toxicity of the material. Holographic performance of the NIPA-based photopolymer in both transmission and reflection modes was characterized and the optimum recording conditions at the spatial frequency of 300, 1000 and 2700 lines/mm in transmission mode and 2700 lines/mm in reflection mode were identified. In addition to fulfilling the requirements for holographic recording materials, the NIPA-based photopolymer is sensitive to temperature. Characteristics of holographic gratings recorded in the NIPA-based photopolymer are found to be temperature dependent. Temperature-induced changes of the diffraction efficiency of transmission gratings and the wavelength shift of reflection gratings are reversible within 2 % and 5 nm, respectively. The temperature response of holographic gratings can be used for the development of holographic temperature sensors operating in transmission or reflection mode.

Acknowledgment. This work was partially funded by Enterprise Ireland (Grant CF20133307) and co-funded by the European Regional Development Fund under Ireland's European Structural and Investment Funds Programmes 2014-2020 and the Irish Research Council.

References

1. M. Zawadzka, T. Mikulchyk, D. Cody, S. Martin, A. K. Yetisen, J. L. Martinez-Hurtado, H. Butt, E. Mihaylova, H. Awala, S. Mintova, S. H. Yun, and I. Naydenova, "Photonic Materials for Holographic Sensing," in *Photonic Materials for Sensing, Biosensing and Display Devices*, M. Serpe, Y. Kang, and Q. Zhang, eds. (Springer International Publishing, 2016), pp. 315-360.
2. A. K. Yetisen, I. Naydenova, F. Vasconcellos, J. Blyth, and C. R. Lowe, "Holographic sensors: Three-dimensional analyte-sensitive nanostructures and their applications," Chem. Rev. **114**, 10654-10696 (2014).
3. R. Bently, *Handbook of Temperature Measurement* (New York: Springer, 1998).
4. J. Blyth, C. R. Lowe, A. G Mayes, and R. B. Millington, "Holographic sensors and their production," Google Patents WO 2004081546 A1 (1999).
5. S. Kabilan, J. Blyth, M. C. Lee, A. J. Marshall, A. Hussain, X. P. Yang, and C. Lowe, "Glucose-sensitive holographic sensors," J. Mol. Recognit. **17**, 162-166 (2004).
6. I. Naydenova, H. Sherif, S. Martin, R. Jallapuram, and V. Toal, "Holographic sensor," Google Patents US8535853 B2 (2013).
7. H. Liu, D. Yu, K. Zhou, D. Mao, L. Liu, H. Wang, W. Wang, and Q. Song, "Temperature-induced spectrum response of volume gratings as an effective stragedy for holographic sensing in acrylamide polymer. Part 1:sensing," Appl. Opt. **55**, 9907-9916 (2016).
8. D. Mao, Y. Geng, H. Liu, K. Zhou, L. Xian, and D. Yu, "Two-way shift of wavelength in holographic sensing of organic vapor in nanozeolites despersed acrylamide photopolymer," Appl. Opt. **55**, 6212-6221 (2016).
9. D. E. Lucchetta, L. Criante, and F. Simoni, "Optical characterization of polymer dispersed liquid crystals for holographic recording," J. Appl. Phys. **93**, 9669-9674 (2003).
10. L. De Sio, N. Tabiryan, and T. Bunning, "POLICRYPS-based electrically switchable Bragg reflector," J. Opt. Express **23**, 32696-32702 (2015).
11. T. Bunning, L. Natarajan, V. Tondiglia, and R. Sutherland, "Holographic polymer-dispersed liquid crystals (H-PDLCs)," Annu. Rev. Mater. Sci. **30**, 83-115 (2000).
12. R. Caputo, L. De Sio, A. Veltri, C. Umeton, and A.V. Sukhov, "Development of a new kind of switchable holographic grating made of liquid-crystal films separated by slices of polymeric material," Opt. Lett. **29**, 1261-1263 (2004).
13. J.V. Crivello and E. Reichmanis, "Photopolymer materials and processes for advanced technologies," Chem. Mater. **26**, 533-548 (2014).
14. M. V. Deshmukh, A. A. Vaidya, M. G. Kulkarni, P. R. Rajamohanan, and S. Ganapathy, "LCST in poly(*N*-isopropylacrylamide) copolymers: high resolution proton NMR investigations," Polymer **41**, 7951-7960 (2000).
15. K. Hashimoto, J. Sakamoto, and H. Tanii, "Neurotoxicity of acrylamide and related compounds and their effects on male gonads in mice," Arch. Toxicol. **47**, 179-189 (1981).
16. H. Tanii and K. Hashimoto, "Neurotoxicity of acrylamide and related compounds in rats," Arch. Toxicol. **54**, 203-213 (1983).
17. M. Islam, A. Ahiabu, X. Li, and M. Serpe, "Poly (N-isopropylacrylamide) Microgel-Based Optical Devices for Sensing and Biosensing," Sensors **14**, 8984-8995 (2014).
18. J. Kopeček, "Smart and genetically engineered biomaterials and drug delivery systems," Eur. J. Pharm. Sci. **20**, 1-16 (2003).
19. K. T. Nguyen and J. L. West, "Photopolymerizable hydrogels for tissue engineering applications," Biomaterials **23**, 4307-4314 (2002).
20. P. Ravichandran, K. L. Shantha, and K. P. Rao, "Preparation, swelling characteristics and evaluation of hydrogels for stomach specific drug delivery," Int. J. Pharm. **154**, 89-94 (1997).
21. I. Craciunescu, A. Nan, R. Turcu, I. Kacso, I. Bratu, C. Leostean, and L. Vekas, "Synthesis, characterization and drug delivery application of the temperature responsive pNIPA hydrogel," JPCS **182**, 012060 (2009).
22. K. Haraguchi, T. Takehisa, and M. Ebato, "Control of cell cultivation and cell sheet detachment on the surface of polymer/clay nanocomposite hydrogels," Biomacromolecules **7**, 3267-3275 (2006).
23. Q. Gong, S. Wang, M. Huang, and F. Gan, "A humidity-resistant highly sensitive holographic photopolymerizable dry film," Mater. Lett. **59**, 2969-2972 (2005).
24. T. Mikulchyk, S. Martin, and I. Naydenova, "Investigation of the sensitivity to humidity of an acrylamide-based photopolymer containing *N*-phenylglycine as a photoinitiator," Opt. Mater. **37**, 810-815 (2014).
25. D. Cody, I. Naydenova and E. Mihaylova, "Effect of glycerol on a diacetone acrylamide-based holographic photopolymer material," Appl. Opt. **53**, 489-494 (2013).

26. E. Leite, *Photopolymerizable Nanocomposites for Holographic* Applications, (Doctoral Thesis, Dublin Institute of Technology, 2010).
27. E. Mihaylova, D. Cody, I. Naydenova, S. Martin, and V. Toal, "Diacetone-acrylamide based pressure sensitive photopolymer," British Patent Application No. GB1411640.4 (2014).
28. T. Furuncuoğlu, İ. Uğur, İ. Değirmenci, and V. Aviyente, "Role of chain transfer agents in free radical polymerization kinetics," Macromolecules **43**, 1823-1835 (2010).
29. S. Martin, I. Naydenova, R. Jallapuram, R. G. Howard, and V. Toal. "Two way diffusion model for the recording mechanism in a self-developing dry acrylamide photopolymer", Proc. SPIE **6252**, 625205-625205-8S (2006).
30. T. Babeva, I. Naydenova, D. Mackey, S. Martin, and V. Toal, "Two-way diffusion model for short-exposure holographic grating formation in acrylamide-based photopolymer," JOSA B **27**, 197-203 (2010).
31. J. Raghavendra, *Optimisation of an acrylamides-based photopolymer for reflection holographic recording*, (Doctoral Thesis,. Dublin : Dublin Institute of Tecnology, 2005).
32. D. Cody, S. Gribbin, E. Mihaylova, and I. Naydenova, "Low-toxicity photopolymer for reflection holography," ACS Appl. Mater. Interfaces **8**, 18481-18487 (2016).
33. H. Kogelnik, "Coupled wave theory for thick hologram gratings," Bell Syst. Tech. J. **48**, 2909-2947 (1969).
34. P. Phariseau, "On the diffraction of light by progressive supersonic waves," Proc. Indiana Acad. Sci. A **44**, 165-170 (1956).
35. S. Gallego, M. Ortuño, C. Neipp, A. Marquez, A. Belendez, I. Pascual, J.V. Kelly, and J.T. Sheridan, "Physical and effective optical thickness of holographic diffraction gratings recorded in photopolymers," Opt. Express **13**, 1939 (2005).
36. H. Wang, J. Wang, H. Liu, D. Yu, X. Sun, and J. Zhang, "Study of effective optical thickness in photopolymer for application," Opt. Lett., **37**, 2241-2243 (2012).
37. H. Wang, S. Xu, J. Ma, Z. Wang, and E. Hou, "Investigation of high thickness holographic gratings in acrylamide-based photopolymer," Mod. Phys. Lett. B **30**, 1650382 (2016).